Superconductor
Science and
Technology

PAPER

CORC® wires allowing bending to 20 mm radius with 97.5% retention in critical current and having an engineering current density of 530 A mm^{-2} at 20 T

To cite this article: Danko van der Laan *et al* 2024 *Supercond. Sci. Technol.* **37** 115007

IOP Publishing Superconductor Science and Technology
Supercond. Sci. Technol. **37** (2024) 115007 (16pp) https://doi.org/10.1088/1361-6668/ad7c89

CORC® wires allowing bending to 20 mm radius with 97.5% retention in critical current and having an engineering current density of 530 A mm^{-2} at 20 T

Danko van der Laan[1,2,*], **Jeremy Weiss**[1,2], **Kyle Radcliff**[1] and **Dmytro Abraimov**[3]

[1] Advanced Conductor Technologies LLC, Boulder, CO 80301, United States of America
[2] University of Colorado, Boulder, CO 80309, United States of America
[3] Applied Superconductivity Center, National High Magnetic Field Laboratory, Florida State University, Tallahassee, FL 32310, United States of America

E-mail: danko@advancedconductor.com

Received 27 July 2024, revised 25 August 2024
Accepted for publication 18 September 2024
Published 27 September 2024

Abstract

Low-inductance, high-field insert solenoid magnets and 20 T dipole magnets for particle accelerators require flexible cables, wound from high-temperature superconductors (HTS) such as RE-$Ba_2Cu_3O_{7-}\delta$ (REBCO) coated conductors, that allow bending to a 20 mm radius without significant degradation in performance. They require an operating current of at least 5 kA and a high engineering current density (J_e) exceeding 500 A mm^{-2} at 20 T. HTS cable technologies that target such demanding magnet applications so far have not been able to meet the combination of these requirements. Here we present the development of the next generation of Conductor on Round Core (CORC®) wires that are produced with an optimized manufacturing process that improves their bending flexibility by factor of more than 2 compared to previous generation CORC® wires. CORC® wires now allow for a bending radius of 20 mm with only 2%–3% performance degradation. They allow bending to a radius of 15 mm with a performance retention of 83.5%. The performance of 30-tape CORC® wires wound from 2 mm wide REBCO tapes from SuperPower Inc, SuperOx and shanghai superconductor technologies was measured at magnetic fields up to 12 T. The overall performance at high magnetic fields of the next generation of CORC® wires improved by a factor of 1.5–1.8, depending on the REBCO tape manufacturer. CORC® wires wound from production REBCO tapes achieved a new record J_e of 751 A mm^{-2} at a current of 8.3 kA at 12 T, and a J_e of 530 A mm^{-2} at a current of 5.8 kA when extrapolated to 20 T. The next generation of CORC® wires present the first HTS cable technology that simultaneously meet the requirements on bending flexibility, engineering current density and critical current at 20 T for use in low-inductance, high-field particle accelerator magnets. They now enable a more expedited development of prototype

* Author to whom any correspondence should be addressed.

low-inductance solenoid magnets that target fields exceeding 25 T and of accelerator magnets that generate a dipole field exceeding 20 T.

Keywords: CORC®, wire, bending performance, high field performance

1. Introduction

High-temperature superconductors (HTS) have been widely recognized as an enabling technology for high-field magnets that generate a magnetic field exceeding 20 T, or operate at elevated temperatures above 20 K, which are outside the reach of low-temperature superconductors (LTS). One of the more challenging magnet applications for HTS are low-inductance accelerator magnets that would generate a dipole field of 20 T, and low-inductance solenoid magnets that generate magnetic fields exceeding 25 T. These magnets require very high operating currents of at least 5–10 kA, which is far outside the range of single RE-$Ba_2Cu_3O_{7-\delta}$ (REBCO) and $Bi_2Sr_2Ca_2Cu_3O_x$ (Bi-2223) tapes, or $Bi_2Sr_2CaCu_2O_x$ (Bi-2212) round wires. HTS tapes or wires therefore need to be bundled into high-current cables that are flexible enough to allow winding at a radius of no more than 20 mm without any significant performance degradation. Besides the high operating current and bending requirements, HTS cables should also allow operation at a high engineering current density (J_e) of at least 500 A mm^{-2} at the operating field of at least 20 T to avoid the magnets from becoming extraordinarily large in size [1]. Besides a much higher magnet cost, this would prevent the HTS magnet to be operated within an LTS outsert, as for instance envisioned in hybrid accelerator magnets [2–6].

Several HTS cable technologies are under development for use in low-inductance, high field magnets. Rutherford cables wound from Bi-2212 wires have been demonstrated in small prototype dipole coils generating stand-alone dipole fields of 1.64 T in a canted-cosine theta (CCT) magnet [7], and 3.5 T in a common coil configuration [8]. The intrinsic mechanical weakness of Bi-2212 wires, which is one of the main disadvantages of this material for use in high-field magnets, requires significant external support provided to the magnet windings, which increases the J_e requirements of the cables. Bi-2212 cables can be bent to radii below 30 mm because the superconducting filaments are formed only once the magnet has been wound. The high temperature reaction within a high-pressure furnace to form the Bi-2212 phase [9] requires precise temperature control of the entire coil, and currently forms one of the main barriers preventing high-field magnets based on Bi-2212 cables to become a reality.

Several HTS cable designs based on REBCO coated conductors have been pursued for high-field magnet applications. These include designs that are electrically and mechanically anisotropic, such as Roebel cables in which patterned REBCO tapes are assembled into a highly-aspected transposed cable [10, 11]. They also include the twisted stacked tape cable [12, 13] and stacked tape cables in which the stack is not twisted. Roebel cables cannot be freely bent in all directions, allowing bending to a radius of less than 16 mm in the 'easy' direction, while they do not allow bending in the 'hard' direction. They also suffer from a high sensitivity to external loads oriented along the tape plane [14]. As a result, only limited success in high-field accelerator magnets has been achieved with roebel cables, in which stand-alone dipoles field of 3.1 T have been reached at 6.5 kA [15–17].

REBCO tape based HTS cables also include fully isotropic cables, allowing bending in all directions, in which the REBCO tapes are wound into a helical fashion around a small round core, such as Conductor in Round Core (CORC®) cables [18, 19] and wires [20, 21]. The helical wind in CORC® cables and wires makes their electrical performance independent on the applied magnetic field angle, while their mechanical response to external stresses is independent of the direction at which the stress is applied, making them a highly attractive option for high-field magnets.

The development of CORC® wires for high-field accelerator magnets focusses on optimizing the bending flexibility while at the same time maximizing J_e. CORC® wires now typically contain 30 REBCO tapes of 2 mm width that contain 30 μm substrates, wound around a 2.55 mm solid copper core, resulting in an overall conductor diameter of about 3.7 mm [22]. Until recently, CORC® wires allowed bending to a 30 mm radius at an acceptable, but not ideal performance degradation of around 20%–25% [20, 22]. They achieved a J_e extrapolated to 20 T of around 300 A mm^{-2} when wound from production REBCO tapes, or over 450 A mm^{-2} using research tapes with record performance and substrate thickness of 25 μm [21].

STAR® wires also present a REBCO cable in which the tapes are wound in a helical fashion around a small core [23]. They differentiate from CORC® wires in that they are based on R&D tapes in which the REBCO layer is moved closer to the neutral axis of the tape by using asymmetric copper plating. This allows the use of even thinner cores of 0.5–0.8 mm, resulting in a higher short-sample J_e at 20 T of 586 A mm^{-2}. Thinner cores come with potential challenges because the resilience of helical-wound REBCO cables under transverse compressive load is limited by the conductor core size. CORC® conductors degrade at a transverse compressive load of about 100 kN m^{-1} and 240 kN m^{-1} when containing cores of 2.55 mm and 3.2 mm thickness, respectively [24]. Significant deformation of the STAR® wire core was indeed observed after testing at 2.5 kA in 30 T background field [25], which corresponds to a transverse load of 75 kN m^{-1} . Increasing the operating current of STAR® wires to exceed 3–4 kA at 20 T currently requires multiple STAR wires to be wound in parallel to achieve the high operating currents needed for low-inductance magnets [26, 27].

Development of CORC® conductors based on production REBCO tapes already resulted in the successful demonstration

of a high field insert solenoid magnet that generated a peak magnetic field of 16.77 T at a current of 4.4 kA within a 14 T LTS outsert solenoid [28]. The insert coil was wound from a 4.5 mm thick CORC® wire that allowed bending to a limited bending radius of 50 mm and resulted in a J_e at 16.77 T of only about 282 A mm^{-2}. Although the CORC® wire performance did not meet the requirements for high-field accelerator magnets, the degradation-free insert coil test presented an important milestone for CORC® conductors for high-field magnet applications. Several prototype CCT dipole magnets have been developed by Lawrence Berkeley National Laboratory, which stand-alone dipole fields of 1.1 T [29] and 2.9 T [22] have been demonstrated. The 2.9 T CCT magnet operated at a current of 6.29 kA and was based on a minimum bending radius at the poles of 30 mm, where the CORC® wire demonstrated a retention in critical current (I_c) of about 75%–80%. A 5 T CCT magnet is currently being wound from 145 meters of 30-tape CORC® wire, containing about 7.5 km of SuperPower (SP) 'HM' REBCO tape, which is optimized for high-field operation. While R&D tapes allow record performance in short HTS cables as a proof-of-principle, the high tape lengths required for prototype accelerator magnets emphasizes the importance that the strict bending and operating performance of HTS cables needs to be achieved using production REBCO tapes.

In this paper, we address the two remaining barriers that prevent rapid development of high-field accelerator magnets that would achieve dipole fields of 20 T using CORC® wires: their limited bending flexibility and their limited in-field performance when wound from production REBCO tapes. Besides CORC® wire core size and REBCO tape width, friction between tapes in CORC® wires is responsible for most bending degradation [30]. The effect on the bending performance of an optimized CORC® wire lubrication and winding process that minimizes friction between tapes will be presented using 2 mm wide REBCO tapes with 30 μm substrate available at commercial lengths from SP Inc., SuperOx (SO, recently rebranded as Faraday Factory), and Shanghai Superconductor Technologies (SST). The performance of optimized CORC® wires wound from 30 production REBCO tapes from the three vendors is measured at magnetic fields up to 12 T to demonstrate the CORC® wire's ability to achieve an operating current exceeding 5 kA and a J_e exceeding 500 A mm^{-2} when extrapolated to 20 T.

2. Experimental

2.1. Sample preparation

The approach to improve the bending flexibility of CORC® wires focused on reducing the friction between tapes by optimizing the lubricant and lubricant application method in combination with optimization of the CORC® wire winding parameters. The exact details of how the friction between tapes is reduced is considered a trade secret and will not be disclosed in this paper. The initial optimization of the original manufacturing process (Process P1) resulted in Process P2, while further optimization resulted in Process P3.

The REBCO tapes for winding CORC® wires were purchased commercially from three manufacturers. All tapes were slit to 2 mm width, contained Hastelloy C-276 substrates of 30 μm thickness, and plated copper layers of 5 μm in thickness. The 1.6–1.8 μm thick REBCO layer of tapes from SP Inc. Produced by metal-organic chemical vapor deposition using their latest 'HM' formulation aimed at low-temperature operation at high magnetic field. Two variations of tapes were purchased from SO : one containing a 1.5 μm, and one containing a 2.5 μm thick REBCO layer, both produced using pulsed-laser-deposition (PLD) and optimized for low-temperature, high-field operation. The 2 μm thick REBCO layer of the tapes from SST was also produced with PLD but was not optimized for high-field application.

Table 1 lists the layout of the three CORC® wires wound from 30 REBCO tapes from the three vendors. The main difference between the three layouts is that the CORC® wire wound from SO tapes with a 2.5 μm thick REBCO layer contained a 3.2 mm thick solid copper core, resulting in a 4.15 mm thick CORC® wire. The CORC® wires wound from SP and Shanghai Superconductor tapes contained a 2.55 mm thick copper core, resulting in a final thickness of 3.66–3.8 mm. The table includes the expected CORC® wire I_c at 76 K based on the average and minimum I_c of the REBCO tapes before cabling.

2.2. Measurement procedure

Two methods were used to determine the effect of bending on the CORC® wire performance. The first method consisted of measuring the I_c in liquid nitrogen at 76 K of the 30-tape CORC® wire at different bending radii (figure 1). The voltage versus current (*VI*) characteristic was measured using voltage wires that were incorporated between the terminations and the CORC® wire, while I_c was defined at an electric field criterion of 1 μV cm^{-1} . This method tends to underestimate the bending degradation, because the self-field effect at the high-current terminations typically results in a I_c value that's about 80% of the I_c determined from a summation of the individual tape I_cs. The self-field effect at the terminations therefore hides the initial I_c degradation at the bent section of the CORC® wire [20]. The second method that was applied to determine the extent of I_c degradation due to bending was to bend a 0.1 m long CORC® wire section to a certain radius, after which the REBCO tapes were carefully extracted from the CORC® wire section and their I_c measured. The I_c retention as a function of bending radius was defined as the total tape I_c at a given bending radius normalized to the total I_c of the tapes extracted from a straight CORC® wire section. This method removes any self-field effects of the CORC® wire terminations, and any potential reversible strain effects that me be present in the REBCO tapes after winding onto the small core. It also allows determination of the location within the CORC® wire at which degradation first occurs, guiding further optimization of the CORC® wire layout and winding procedure.

The performance of the CORC® wires was measured at 4.2 K in liquid helium at magnetic fields up to 12 T within a superconducting solenoid magnet (figure 2(a)). The CORC®

Table 1. CORC® wire sample details.

	Unit	Wire-SP	Wire-SO	Wire-SST
REBCO tape manufacturer		SuperPower HM	SuperOx	Shanghai Superconductor
Process		P2	P2	P3
Number of tapes		30	30	30
Tape width	(mm)	2	2	2
Slitting process		Mechanical	Laser	Laser
Substrate thickness	(μm)	30	30	30
Core thickness	(mm)	2.55	3.2	2.55
CORC® wire thickness	(mm)	3.8	4.15	3.66
Sum of average tape I_c (76 K)	(A)	954.6	3,011	3,051
Sum of minimum tape I_c (76 K)	(A)	928.7	2,195	2,858
Sum of extracted tape I_c (76 K)	(A)	930.7	2,640	2,653

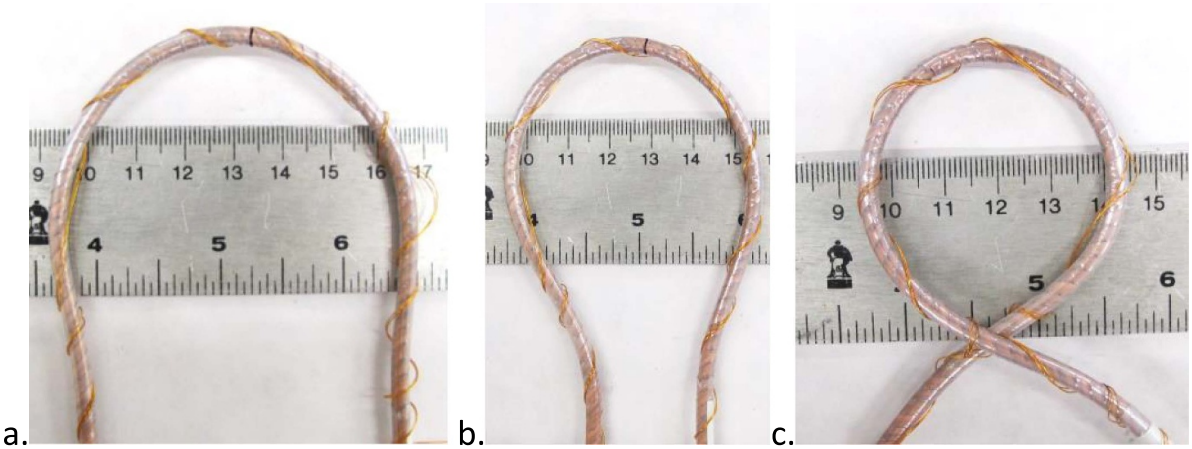

Figure 1. CORC® wire wound from 30 shanghai superconductor tapes (Wire-SST) bent to a radius of (a) 31.5 mm, (b) 25 mm, and (c) 20 mm.

wire sample of about 1.5 meters in length was placed into a grooved mandrel after being bent into a hairpin of either 20 mm radius (Wire-SST), or 31.5 mm radius (Wire-SP and Wire SO) (figure 2(b)). The CORC® wire was secured in place using stycast FT-2850 epoxy. Current was applied to the CORC® wire at different ramp rates between 50 A s^{-1} and 500 A s^{-1} up to 12 kA.

3. Results

3.1. Performance of 2 mm wide REBCO tapes containing 30 μm thick substrates

The critical current as a function of magnetic field of 2 mm wide REBCO tapes containing 30 μm substrates from SP Inc., SO and SST was measured at 4.2 K for magnetic field applied perpendicular to the tape surface (figure 3). REBCO tapes produced by SP with the 'HM' formulation showed a relatively wide variation in I_c of 60%–100% between batches. Their in-field performance below 10 T exceeded that of SO and SST tapes by about 35% and 50%, respectively. The differences in in-field performance between tapes from the three vendors decreased significantly at magnetic fields above 10 T.

The performance of 2 mm wide REBCO tapes with 30 μm substrate was also measured after winding onto different diameter formers to qualify the tapes for winding into CORC® wires. The tapes were each wound onto a round former at an angle of about 45° with the REBCO layer facing inward [19]. SP tape produced using their 'AP' formulation previously allowed cabling onto a 2.3 mm core. Figure 4(a) shows that I_c at 76 K of tapes from some of the SP HM batches already degraded at a relatively large winding diameter of 2.8 mm, while those of other batches demonstrated a comparable bending performance as previous SP 'AP' tapes. Tapes from batches with poor bending performance were not cabled into CORC® wires.

The performance at different winding diameters of SO production tapes containing a 2.5 μm thick REBCO layer is shown in figure 4(b). The smallest former size before irreversible degradation occurred was about 3.0 mm. On the other hand, SO R&D tapes with a REBCO layer of 1.5 μm in thickness allowed cabling onto formers as small as 2.3 mm. A significant (20%), but fully reversible decrease in I_c occurred in SO tapes during winding. The open symbol in figure 4(b) shows that I_c fully recovers when the tape is straightened after it was first wound to 5 mm diameter. Figure 4(c) shows

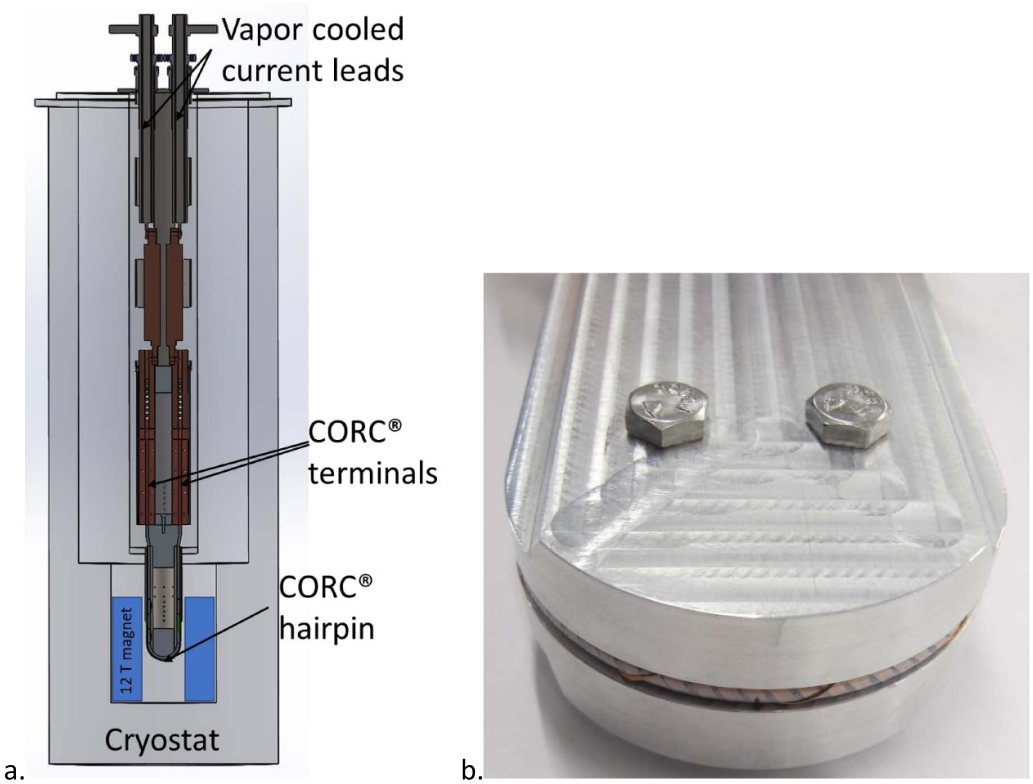

Figure 2. (a) cross-section of test setup for testing CORC® wires at 4 K in magnetic fields up to 12 T. (b) Closeup of the CORC® wire in a 31.5 mm radius hairpin bend before filling with stycast epoxy.

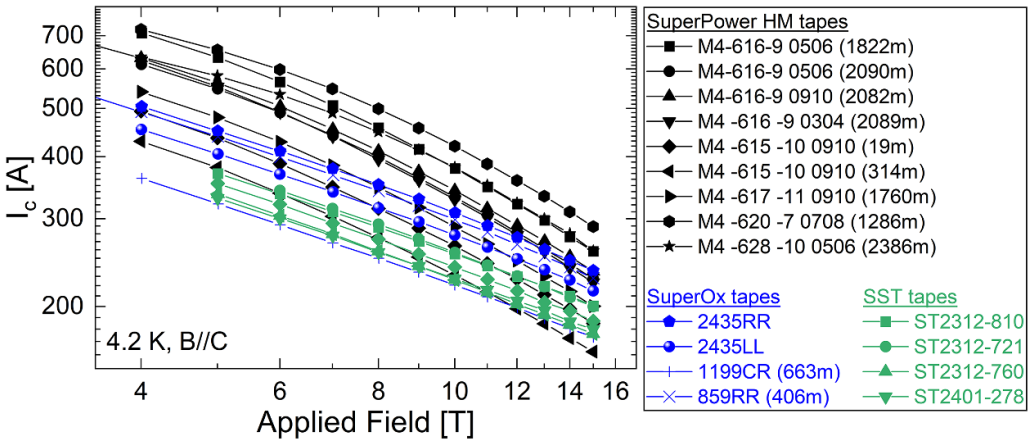

Figure 3. Performance at 4 K of 2 mm wide tapes with 30 μm substrate of superpower 'HM' tapes, superOx and shanghai superconductor technologies tapes, measured as a function of magnetic field applied perpendicular to the tape surface.

the I_c retention of 2 mm wide tapes from several batches of SST tape, allowing cabling to diameters below 2.6 mm, similar to the better performing SP HM tapes shown in figure 4(a).

3.2. Bending performance of next generation of CORC® wires

3.2.1. Bending flexibility of CORC® wires wound from SP HM tapes. The initial improvement of the bending flexibility was performed on 30-tape CORC® wires wound from *SP* 'HM' tapes (Wire-SP in table 1). Figure 5(a) shows the electric field versus current (*EI*) characteristic at different bending radii of a CORC® wire produced with optimized lubrication and winding Process P2. Only a slight shift in *EI*-curve to lower current occurred for a bending radius below 25 mm. Figure 5(b) compares the I_c retention at different bending radii as determined from both full CORC® wire I_c tests and the extracted tape measurements performed on bent CORC® wire sections.

Figure 6(a) shows the I_c of tapes extracted from a straight CORC® wire section (Wire-SP), while figure 6(b) shows their

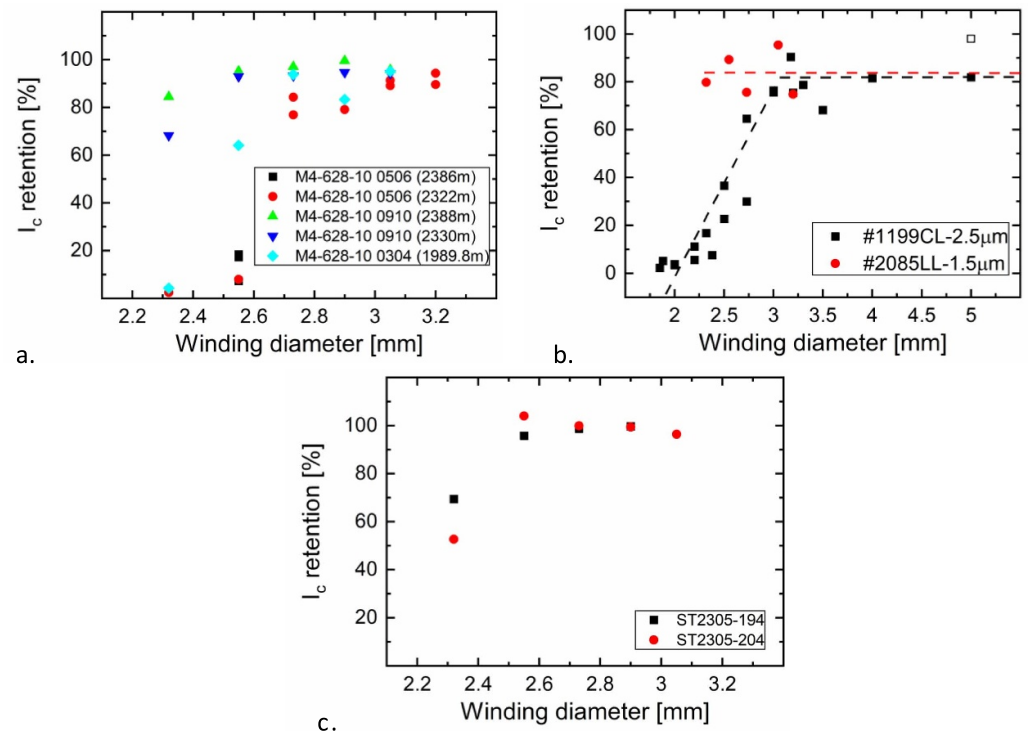

Figure 4. Critical current retention at 76 K of 2 mm wide (a) SuperPower HM, (b) SuperOx, and (c) shanghai superconductor technologies tapes wound at different former diameters. The open symbol in (b) shows the I_c retention of a SO tape that was wound to 5 mm diameter and straightened again. The legends list the tape batch numbers.

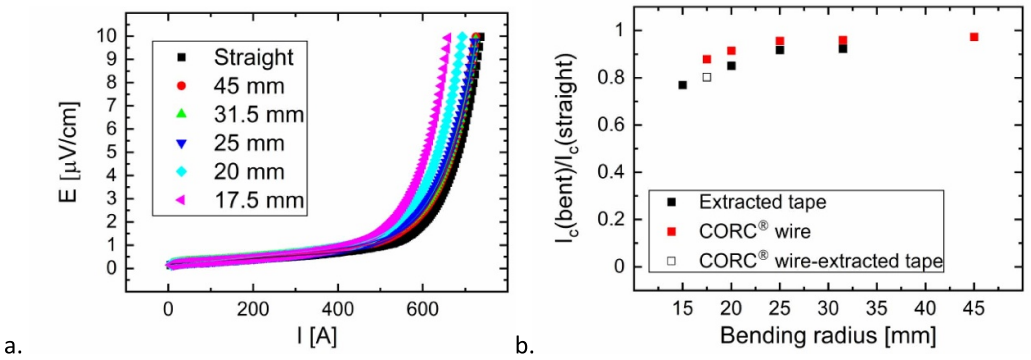

Figure 5. (a) Electric field as a function of current of sample Wire-SP, manufactured with Process P2, at 76 K when bent to different radii. (b) Retention in critical current as function of bending radius and the tapes extracted from the CORC® wire sections bent to specific radii. Also shown is the retention in I_c of tapes extracted from the short CORC® wire after it was bent to a 17.5 mm radius (open symbol).

n-value resulting from fitting the VI-curves using the following equation:

$$V = IR + V_c\left(\frac{I}{I_c}\right)^n, \tag{1}$$

where R is the contact resistance and V_c is the voltage contact separation (L) multiplied by the electric field criterion (E_c) of 1 μV cm^{-1} . Figure 6(a) clearly shows the different I_c of the tapes from different batches wound into layers 5–12, while the tapes in layers 1–4 came from the same batch and all have similar I_cs. One of the tapes extracted from layer 2 was damaged during mounting and had a very low I_c. The n-values for most layers remain above 20, as expected for pristine SP HM tapes, except for some of the tapes of the inner two layers in which the tapes degraded. Figure 6(c) shows the I_c retention of two short CORC® wire sections, one produced with the original process before optimization (Process P1) and the other with Process P2, after bending to a radius of 25 mm. Based on extracted tape measurements, Process P2 resulted in an I_c retention at 25 mm radius of 91.8%, compared to 70% for Process P1. Process P2 resulted in an I_c retention of 80.3% at a bending radius of 17.5 mm, and 77% at a bending radius of 15 mm. Table 2 shows that the I_c retention of the CORC® wire at each

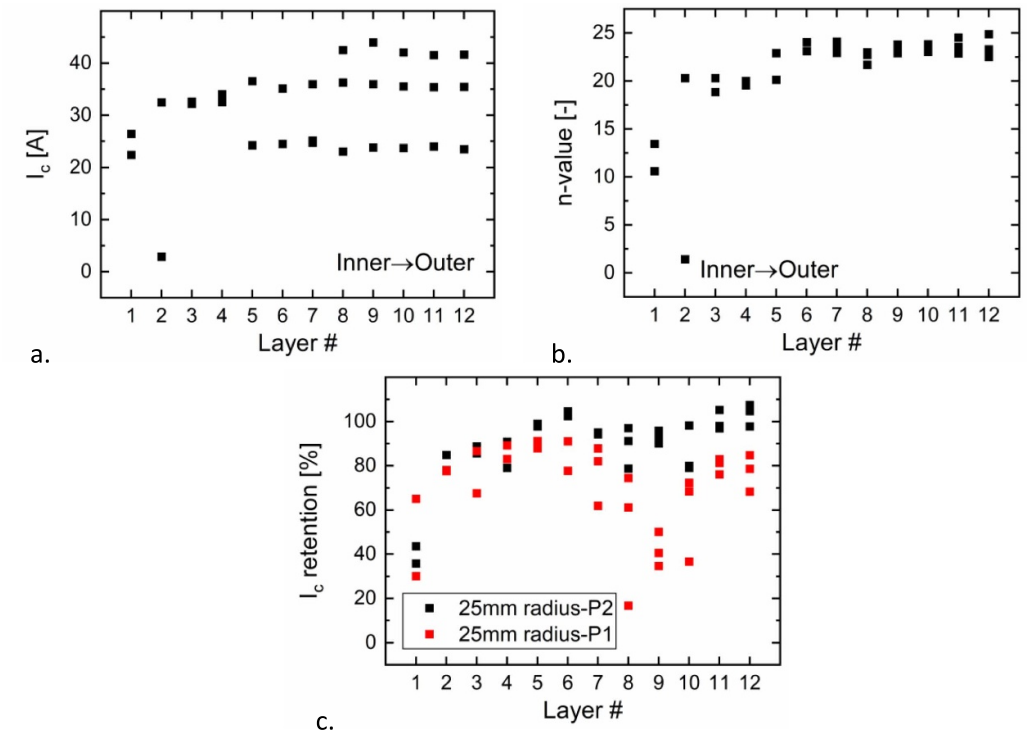

Figure 6. (a) Critical current, and (b) *n*-value as a function of layer number of tapes extracted from a straight CORC® wire section of sample Wire-SP. (c) Critical current retention of a bent CORC® wire sections (Wire-SP) produced with different procedures after bending to 25 mm radius. (I_c retention of 70% for process P1 and 91.8% for process P2).

bending radius is higher than that of the extracted tapes, which is caused by the self-field effect hiding some of the initial bending degradation.

3.2.2. Bending flexibility of CORC® wires wound from SO tapes. The next 30-tape CORC® wire that was prepared using the optimized lubrication and winding Process P2 was wound from production SO tapes (Wire-SO in table 1). Figure 7 shows the *EI*-characteristic and I_c retention at different bending radii, where a small degradation of 9% in I_c was measured once the wire was bent to a 31.5 mm radius and 13% when bent to a 25 mm radius (table 3).

Figure 8 shows the I_c and *n*-value of the tapes extracted from the straight and bent sections of the CORC® wire after the final bending test was completed. The tapes were not flatted after extraction but left in their curled state. Three tapes in layers 1, 3 and 6 burned during the extracted tape measurement at a current far below I_c. Instead of I_c, the highest current before burnout is plotted in figure 8(a) and used to calculate the expected overall CORC® wire I_c before bending. The spread in tape I_c within each layer comes from the two different tape batches used in these layers, each having a slightly different I_c. For the bent section, a spread of about 40% in tape I_c was measured in most layers. The outermost tape layer showed much higher degradation, both in I_c and in *n*-value, which is likely due to the use of a thicker core in the CORC® wire, which requires a higher bending force and thus pressure on the wire. An overall tape I_c retention of 86.5% was measured at a bending radius of 25 mm.

3.2.3. Bending flexibility of CORC® wires wound from shanghai superconductor tapes. The bending performance was measured of CORC® wires wound from SST tape (Wire-SST in table 1) manufactured after further optimization using Process P3. Figure 9 and table 4 show that at a radius of 20 mm, an I_c retention of the CORC® wire of 93.9% was achieved. Tapes extracted from the bent sections of the CORC® wire resulted an I_c retention of 97.5% at that radius (figure 10(b)). This is a higher I_c retention than based on bending the full CORC® wire, suggesting that the initial decrease in CORC® wire I_c at 20 mm radius is due to the increased self-field experienced by the CORC® wire at such small bending radius and does not reflect bending degradation. Some degradation is seen in tapes extracted from the inner and outer layers of the straight CORC® wire. A section of CORC® wire sample Wire-SST was also bent to a radius of 15 mm (figure 10(c)), after which the tapes were extracted and an overall I_c retention of 83.5% was measured. Bending degradation initially occurs only in a limited number of tapes spread out throughout the layers, while most tapes retain their full performance.

3.3. Performance of CORC® wires in a background magnetic field

3.3.1. Performance at high magnetic field of a CORC® wire wound from SP HM tapes. The voltage versus current characteristics of a CORC® wire wound from SP HM tapes (Wire-SP) were measured at different magnetic fields at 4.2 K (figure 11) using a pair of co-wound voltage contacts that were

Table 2. Bending performance of CORC® wire sample Wire-SP manufactured with process P2.

Bending radius (mm)	I_c (A)	n-value —	I_c retention (%)	I_c retention (extracted tapes) (%)
Straight	601.6	10.8	100	100
45	585.3	10.0	97.2	—
31.5	577.3	9.3	96.0	92.4
25	575.3	9.3	95.6	91.8
20	550.4	9.3	91.5	85.1
17.5	529.0	9.7	87.9	80.3
15	—	—	—	77.0

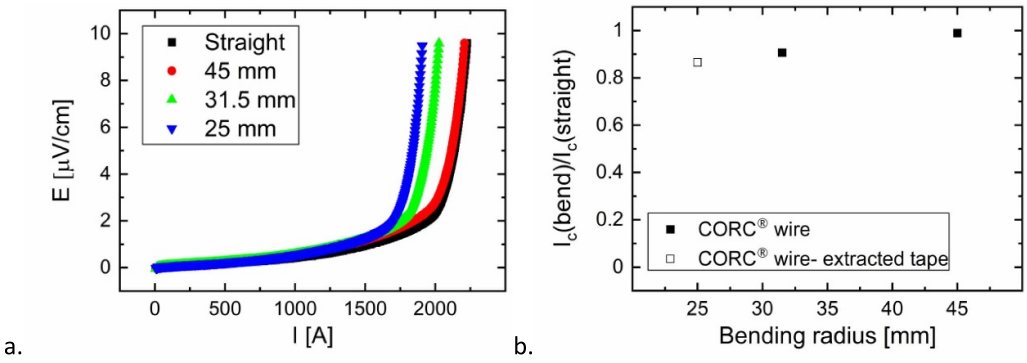

Figure 7. (a) Electric field as a function of current of sample Wire-SO, manufactured with Process P2, at 76 K when bent to different radii. (b) Critical current, normalized to I_c of the straight wire, as a function of bending radius. The open symbol represents the I_c retention determined from extracted tape data, which overlaps the data point of the CORC® wire bent to 25 mm.

Table 3. Bending performance of CORC® wire sample Wire-SO, manufactured with process P2.

Bending radius (mm)	I_c (A)	n-value —	I_c retention (%)	I_c retention (extracted tapes) (%)
Straight	1992	18.7	100	—
45	1973	17.8	99.0	—
31.5	1807	18.0	90.7	—
25	1725	20.6	86.7	86.5

mounted within the terminations of the CORC® wire. The first measurement was taken in a background magnetic field of 9 T at current ramp rates of 100, 200 and 500 A s^{-1}, respectively. The magnetic field was then increased stepwise to 12 T, and finally decreased to 7 T. The measurements only showed the initial start of the superconducting-to-normal transition before the sample quenched. The quench currents (I_{quench}) of the sample at each current ramp rate and magnetic field are listed in table 5. On the way down from 12 T, except at 8 T, the sample was only tested at a current ramp rate of 500 A s^{-1} due to the level of liquid helium running low. The final measurement was performed at 7 T to a current of 11 273 A, at which point part of the sample was pulled from the sample holder due to the high Lorenz force (figure 12). This confirms that the quench triggers were likely caused by sample movement.

Figure 13 shows the quench current and J_e of the CORC® wire, and the expected I_c based on the performance of the individual tapes for which the in-field performance was measured, as a function magnetic field. A J_e of 751 A mm^{-2} at 12 T was measured, which is a new record for CORC® wires wound from production tapes. The magnetic field dependence of the quench current also allowed extrapolation to a magnetic field of 20 T, where the CORC® wire is expected to have a quench current of 5,855 A and a J_e of 530 A mm^{-2}.

3.3.2. Performance at high magnetic field of a CORC® wire wound from SO tapes. The next sample that was measured in a background magnetic field was a 30-tape CORC® wire wound from SO tape (Wire-SO) that was mounted in a hairpin with a radius of 31.5 mm. The *VI*-characteristics are shown in figure 14 when the sample was tested at a current ramp rate of 500 A s^{-1}, starting at 11 T down to a background magnetic field of 6 T. Table 6 lists the quench current, but also I_c and n-value that we were able to obtain

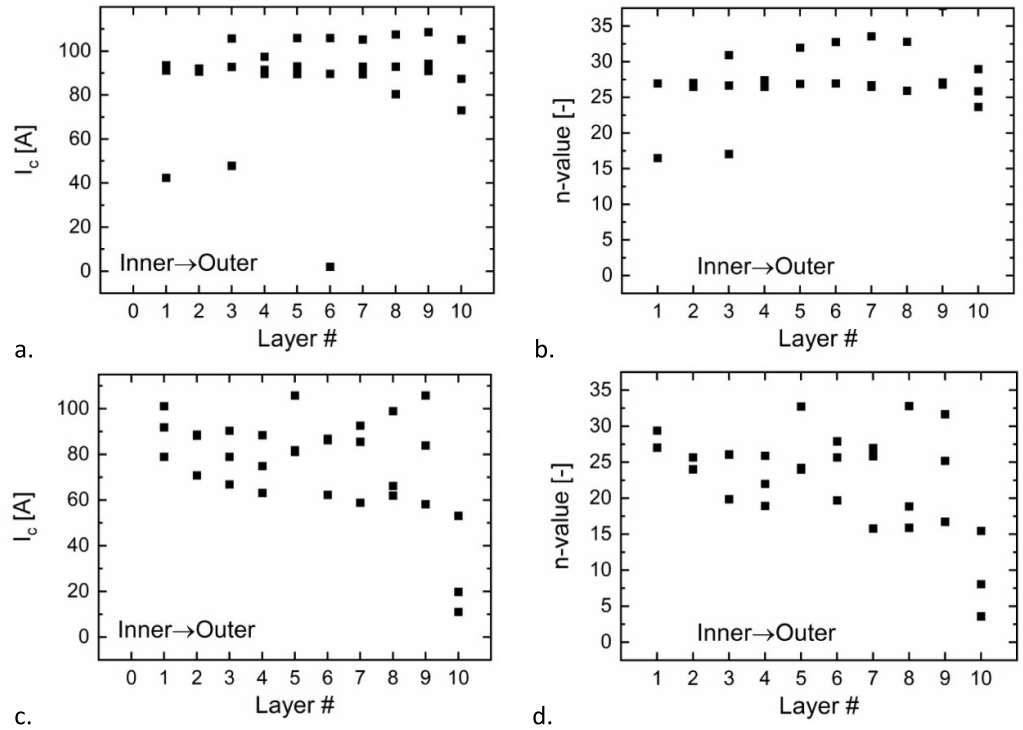

Figure 8. (a) Critical current and (b) n-value as a function of layer number of tapes extracted from a straight section of sample Wire-SO. (c) Critical current and (d) n-value of a CORC® wire section after bending to a 25 mm radius. The total I_c retention at 25 mm radius is 86.5%.

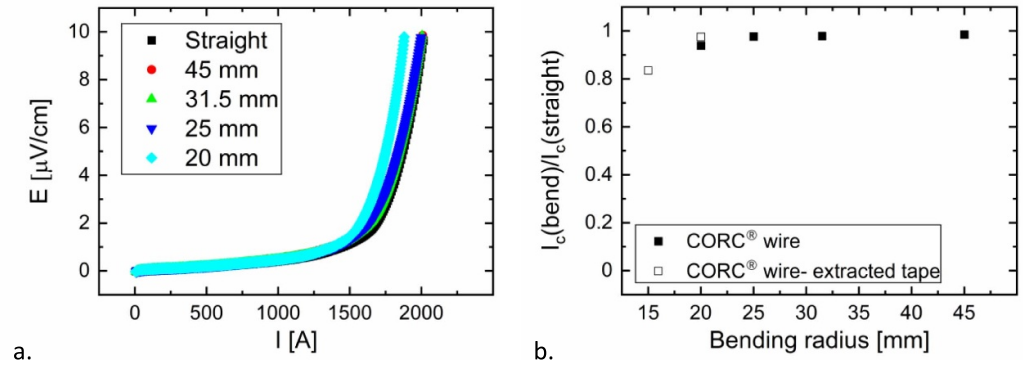

Figure 9. (a) Electric field as a function of current of sample Wire-SST, manufactured with Process P3, at 76 K when bent to different radii. (b) Critical current, normalized to I_c of the straight wire, as a function of bending radius. The open symbol represents the I_c retention determined from extracted tape data.

Table 4. Bending performance of CORC® wire sample Wire-SST, manufactured with Process P3.

Bending radius (mm)	I_c (A)	n-value —	I_c retention (%)	I_c retention (extracted tapes) (%)
Straight	1636	10.4	100	—
45	1611	9.9	98.5	—
31.5	1602	9.8	97.9	—
25	1598	9.7	97.7	—
20	1536	10.8	93.9	97.5
15	—	—	—	83.5

from the limited range at which the voltage showed the superconducting-to-normal transition. This limited voltage range did not allow for an accurate calculation of I_c, therefore the quench current was used to calculate J_e. The actual J_e values are therefore expected to be higher than that listed in table 6.

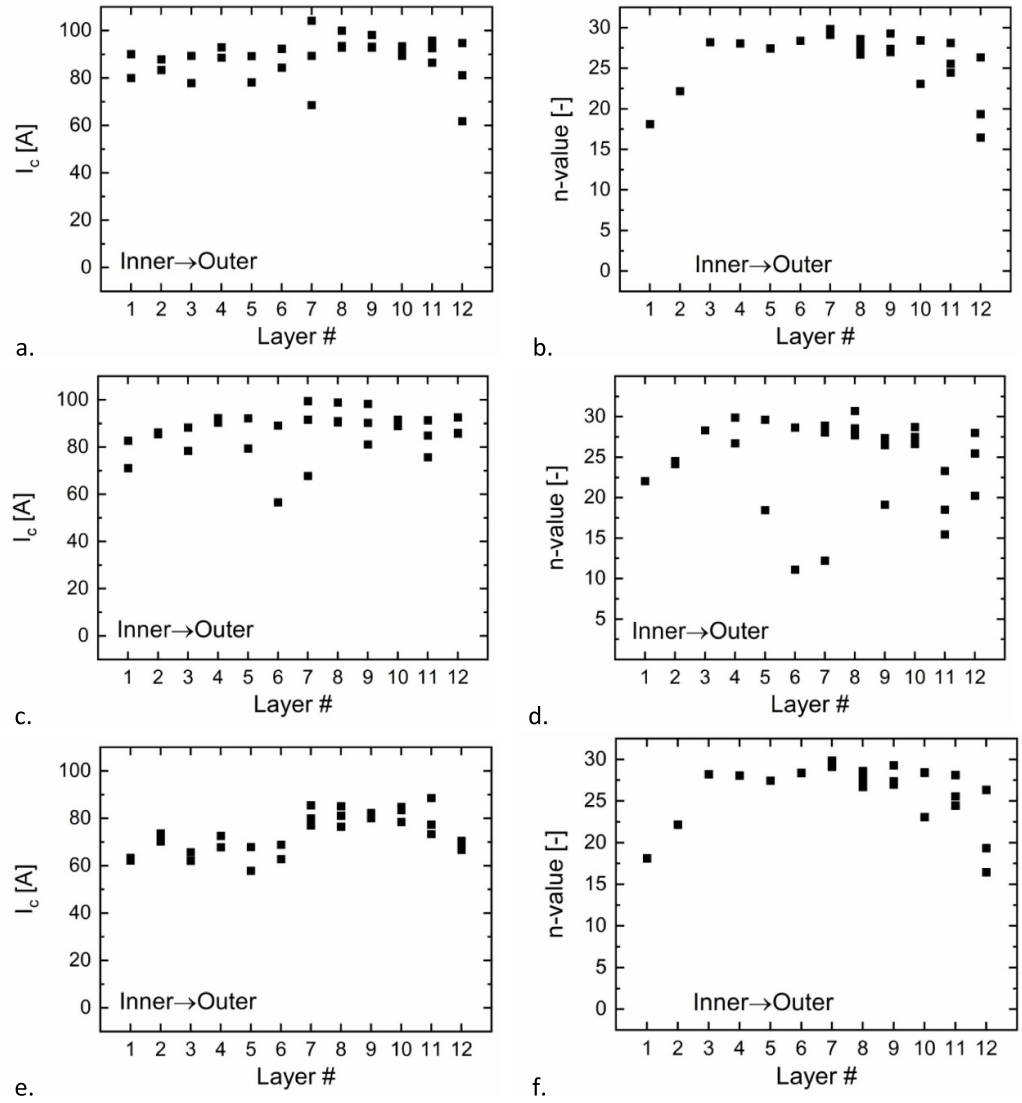

Figure 10. (a) Critical current and (b) *n*-value as a function of layer number of tapes extracted from a straight section of CORC® wire sample Wire-SST, manufactured with Process P3. (c) I_c and (d) *n*-value of a section bent to a radius of 20 mm (I_c retention is 97.5%), and (e) I_c, and (f) *n*-value a section bent to 15 mm radius (I_c retention is 83.5%).

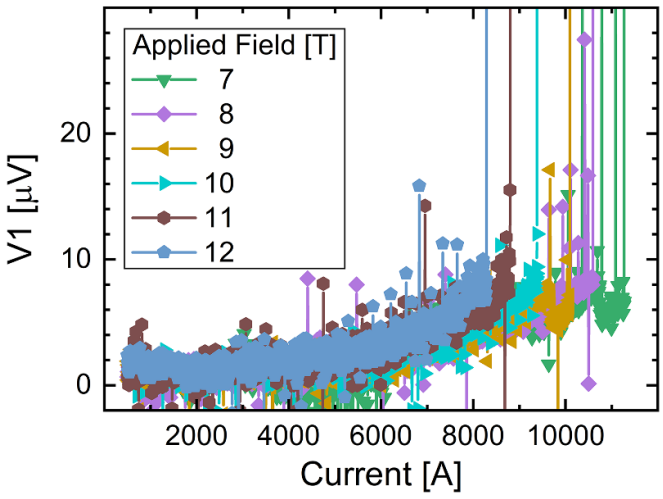

Figure 11. Voltage as a function of current of CORC® wire sample Wire-SP at different magnetic fields at 4.2 K.

Table 5. In-field performance of CORC® wire sample Wire-SP.

B (T)	Sum of tape I_c (A)	I_{quench} (A) 100 (A s^{-1})	I_{quench} (A) 200 (A s^{-1})	I_{quench} (A) 500 (A s^{-1})	J_e (A mm^{-2}) 500 (A s^{-1})
9	12 367	9890	9964	10 098	914
10	11 293	9185	9203	9381	849
11	10 349	8599	8599	8800	797
12	9532		8087	8293	751
11	10 349			8790	796
10	11 293			9421	853
9	12 367			9747	883
8	13 612	10 382	10 568	10 595	959
7	15 016			11 273	1,021
20				5855[a]	530[a]

[a] Extrapolated value.

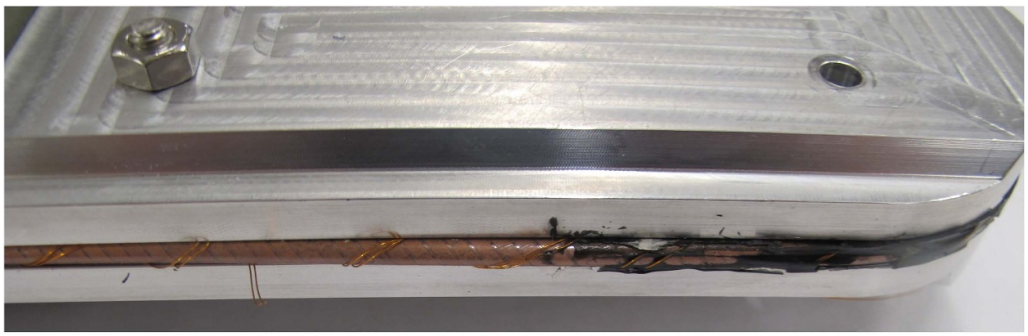

Figure 12. Straight section of CORC® wire Wire-SP on the in-field probe that was pulled from the probe by the high Lorenz force caused by the transverse magnetic field component from the wire's self-field.

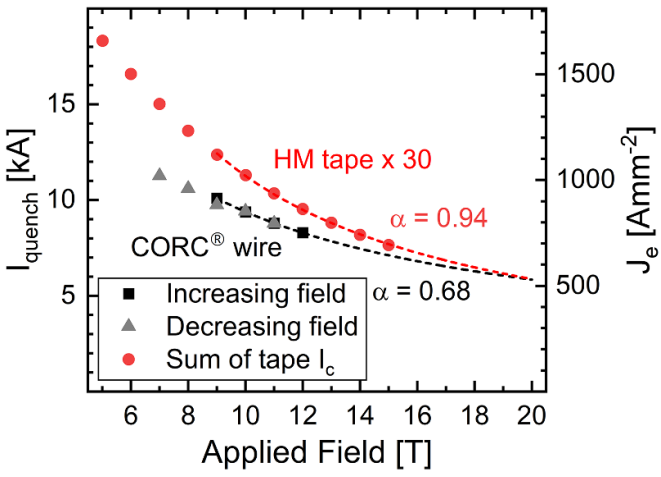

Figure 13. Quench current taken at 500 A s^{-1} and J_e of CORC® wire sample Wire-SP, mounted at 31.5 mm hairpin radius, and total I_c of the tapes from which the CORC® wire was wound, as a function of background magnetic field at 4.2 K. The dashed line is a fit of the quench current to allow extrapolation to 20 T.

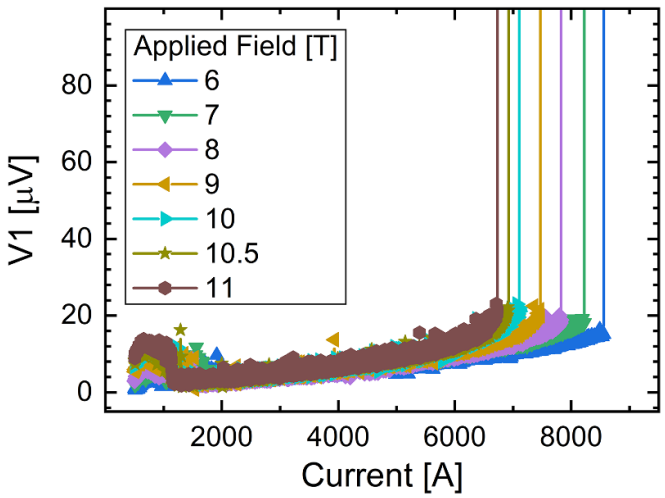

Figure 14. Voltage as a function of current of CORC® wire sample Wire-SO at different magnetic fields at 4.2 K.

Figure 15 shows the quench current of the CORC® wire, and the expected I_c based on the performance of the individual tapes for which the in-field performance was measured. The performance of the CORC® wire at 20 T was estimated by extrapolation, which resulted in an estimated quench current of 5,236 A and J_e of 388 A mm^{-2}. The estimated quench current at 20 T is similar to that of the CORC® wire wound from SP HM tape, but J_e is significantly lower due to the higher thickness of the CORC® wire.

Table 6. In-field performance measured at a current ramp rate of 500 A s^{-1} of CORC® wire sample Wire-SO.

B (T)	Sum of tape I_c (A)	I_{quench} (A)	I_c (A)	n-value	J_e (A/mm^2)
6	11 979	8554	9744	7.7	648
7	11 024	8221	8913	8.3	623
8	10 232	7823	8302	7.8	593
9	9554	7467	7756	7.0	566
10	8970	7108	7232	11.0	538
10.5		6925	7101	11.0	525
11	8460	6731	6883	12.0	510
20		5236[a]			388[a]

[a] Extrapolated value.

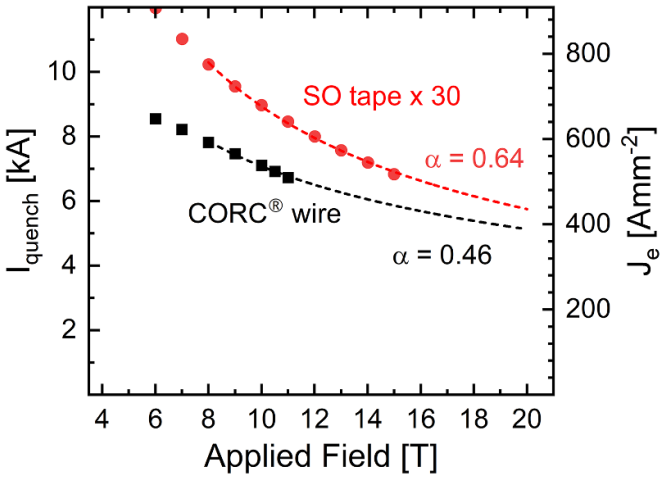

Figure 15. Quench current taken at 500 A s^{-1} and J_e of CORC® wire sample Wire-SO, mounted at 31.5 mm hairpin radius, and total I_c of the tapes from which the CORC® wire was wound, as a function of background magnetic field at 4.2 K. The dashed line is a fit of the quench current to allow extrapolation to 20 T.

3.3.3. Performance at high magnetic field of a CORC® wire wound from Shanghai Superconductor tapes. A CORC® wire wound from SST tape (Wire-SST) was mounted into a hairpin with 20 mm radius for in-field testing. The *VI*-characteristics measured at a ramp rate of 500 A s^{-1} at background magnetic fields from 4 T up to 11 T are shown in figure 16. The current was cycled 10 times to 6,500 A while at 11 T to perform limited stress cycles. No difference in *VI*-characteristics was measured after the stress cycles (figure 17), which indicates that the sample did not degrade during cycling. The performance was measured at 4 T in decreasing field after the measurement at 11 T was performed.

Figure 18 shows the quench current of Wire-SST as a function of background magnetic field, together with the expected I_c based on in-field measurements of several tapes performed up to 15 T. The performance of the CORC® wire is also extrapolated to 20 T, where it is expected to have a quench current of 4,895 A and a J_e of 465 A mm^{-2}. The performance also exceeds the previous CORC® wire J_e(20 T) record reached in 2020 [21] and is only slightly lower than the performance of the CORC® wire wound from SP HM tape.

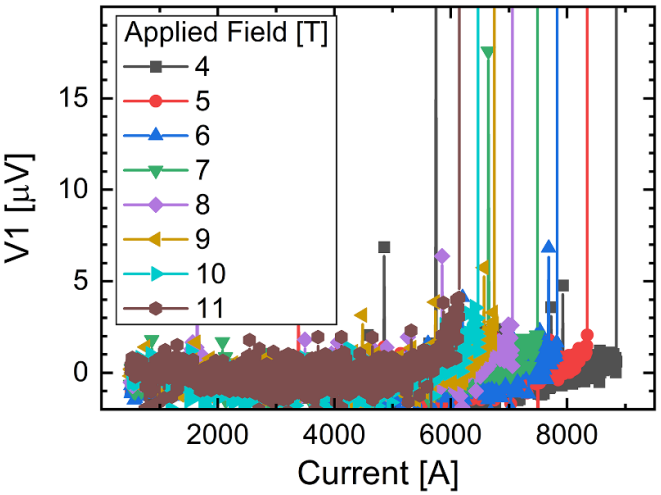

Figure 16. Voltage as a function of current of CORC® wire sample Wire-SST at different magnetic fields at 4.2 K. The measurement was performed at a ramp rate of 500 A s^{-1}.

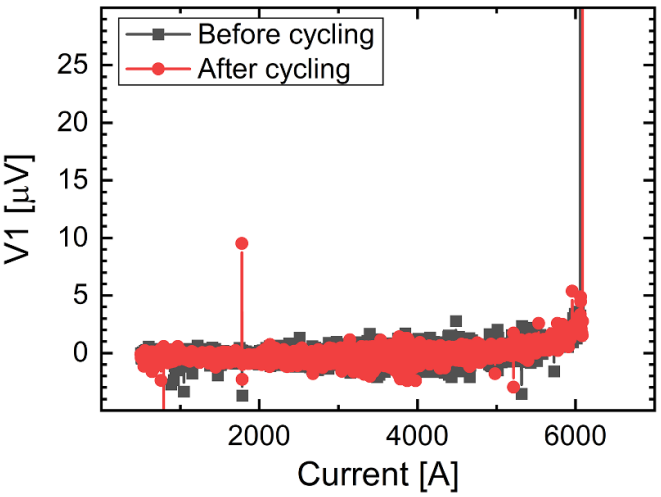

Figure 17. Voltage as a function of current of CORC® wire sample Wire-SST at 11 T and 4.2 K before and after cycling the current 10 times to 6,500 A.

4. Discussion

Table 1 lists the expected CORC® wire I_c of the three samples before bending, based on the average and minimum I_c, as reported by the different vendors, for each tape batch the wires were wound from. At 76 K, the minimum I_c of the SP HM tapes is only slightly below their average I_c, resulting in comparable expected CORC® wire I_c values of 954.6 and 928.7 A, respectively. The total I_c of the tapes extracted from a straight section of CORC® wire sample Wire-SP of 930.7 A fall within the expected range and is only about 2.5% below the expected CORC® wire performance based on

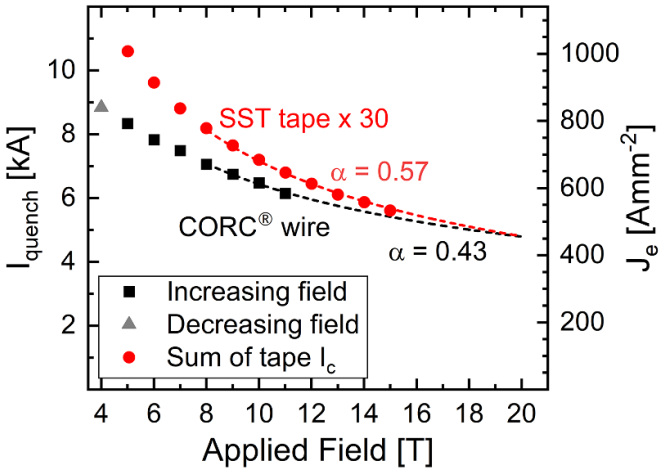

Figure 18. Quench current taken at 500 A s^{-1} and J_e of CORC® wire sample Wire-SST mounted at 20 mm hairpin radius, and total I_c of the tapes from which the CORC® wire was wound, as a function of background magnetic field at 4.2 K. The dashed line is a fit of the quench current to allow extrapolation to 20 T.

the average tape I_c. The much larger variation in I_c along the length of SST, but especially SO tapes, makes it much harder to estimate the expected CORC® wire I_c from the tape performance data provided by the manufacturers. The expected CORC® wire I_c is 3,051 A for sample Wire-SST and 3,011 A for sample Wire-SO at 76 K when based on average tape I_c values. It is only 2,858 A (6.5% less) for sample Wire-SST and 2,195 A (17.2% less) for sample Wire-SO when based on the minimum reported tape I_c. The difference between the expected CORC® wire I_c and the total I_c of the tapes extracted from straight CORC® wire sections of sample Wire-SO and Wire-SST is caused by the wide variation in I_c along the tape length, reversible changes in tape I_c due to cabling (see figure 4(b)), actual irreversible degradation due to cabling, and damage due to tape handling during extraction (the three burned out tapes in figure 8(a)). All these factors, except for tape handing damage, are removed from the equation to evaluate the CORC® wire bending degradation by comparing extracted tape performance between straight and bent CORC® wire sections, which is the method used in this study.

The results presented here clearly show the impact of the reduced friction between tapes on the bending performance of CORC® wires. Before optimization, many of the tapes in the layers around the transition from 2 tapes to 3 tapes per layer (layers 6 and 7) in CORC® wire sample Wire-SP showed significant degradation upon bending (figure 6). This is attributed to the interlayer interaction between tapes within the CORC® wire, as was determined using finite element method modeling to describe similar degradation of the tapes within a CORC® wire exposed to high axial tensile strain [31]. The interlayer interaction is reduced significantly when the friction between tapes is reduced, minimizing the tape degradation in the layers around this transition during bending, as is shown in figure 6 for CORC® wire sample Wire-SP and figure 10 for sample Wire-SST. The reduction in tape degradation around this transition in sample Wire-SO after bending is less pronounced. The sample still shows a wide reduction of tape I_c throughout the sample, likely because of the lower mechanical resilience of the SO tapes against high axial compressive strain during cabling and the use of a thicker core in the CORC® wire.

The quench current of the CORC® wires measured in a background magnetic field varies by no more than 2.5% between current ramp rates ranging from 100 to 500 A s^{-1}. For the case of the CORC® wire wound from SP HM tape (Wire-SP), the quench currents of the two tests performed at 11 T, one before and one after testing at 12 T, were identical. The quench current for sample Wire-SP was higher for the second test performed at 10 T, while it was 3.5% lower for the second test at 9 T. This is not an indication of sample degradation, because the quenches of this sample were likely triggered by sample movement. The quench current of sample Wire-SST decreased by about 2% between the measurements performed at 5 T at the beginning and the end of the test campaign (table 7). This is also unlikely caused by degradation. No change in *VI*-characteristic was measured before and after 10 high current cycles in 11 T background field (figure 17), supporting the claim that no significant degradation occurred in the CORC® wire.

The quench currents of CORC® wires tested in a background magnetic field, and I_c in the case of sample Wire-SO, are lower than expected based on the performance of single tapes. The difference between the expected and actual in-field performance of the CORC® wires is also partly due to the bending degradation experienced by the CORC® wires when wound into the hairpin. The bending tests performed on CORC® wires showed a degradation of around 7% at 31.5 mm radius for sample Wire-SP, which is half of the 13% difference between expected and actual performance at 12 T. The expected bending degradation of about 3% at 20 mm radius for sample Wire-SST is about 1 $3rd^{-1}$ of the 10% difference between expected I_c and CORC® wire quench current measured at 11 T. The bending performance using extracted tape measurements of sample Wire-SO was not performed at a radius of 31.5 mm. Based on the bending performance of the full CORC® wire at a 31.5 mm radius and the 13% I_c degradation at 25 mm radius determined by extracted tape measurements, it is expected that the actual bending degradation of sample Wire-SO at 31.5 mm radius is around 10%. The 18.7% difference between the expected and actual CORC® wire performance at 11 T is therefore not caused entirely be bending degradation but will likely also be caused by the reversible change in tape I_c that was measured when tapes from SO were wound around a small core (figure 4(b)). Although at 76 K this change is close to 20%, the effect will be much lower at 4 K even at fields up to 11 T [32].

The difference between measured and expected in-field performance of the CORC® wires depends on the applied magnetic field. For all CORC® wires tested, the difference between expected and actual in-field performance decreases

Table 7. In-field performance of CORC® wire sample Wire-SST.

B (T)	Sum of tape I_c (A)	I_{quench} (A) 100 (A s^{-1})	I_{quench} (A) 200 (A s^{-1})	I_{quench} (A) 500 (A s^{-1})	J_e (A mm^{-2}) 500 (A s^{-1})
5	10 599	8154	8267	8343	793
6	9620	7648	7726	7831	744
7	8811	7248	7290	7488	712
8	8192	6911	6976	7062	671
9	7647	6593	6671	6745	641
10	7200	6316	6349	6476	616
11	6802	6031	6060	6148	584
5	10 599		8107		
4				8842	840
20				4895[a]	465[a]

[a] Extrapolated value.

with increased magnetic field. This is likely due to the self-field of the CORC® wires being much higher than that of the tapes. The self-field contributions were not considered, and the data shown in figures 13, 15 and 18 are plotted as a function of applied magnetic field, not actual magnetic field experienced by the conductor. The self-field of the CORC® wires wound into a hairpin is mostly oriented perpendicular to the applied magnetic field. Still, the self-field will likely have an effect on the I_c and I_{quench}.

The results presented in this paper show that the bending performance of CORC® wires in which friction between tapes is minimized is still affected by core size and mechanical resilience of the REBCO tapes. The CORC® wire thickness, which is also affected by core size, has a major impact on J_e. On the other hand, a larger core allows for higher layer currents that are needed to reach the required operating current of at least 5 kA at 20 T for use in accelerator magnets. The 2.55 mm core thickness of the standard 30-tape CORC® wires is close to optimum thickness because it allows sufficient bending flexibility in the next generation of CORC® wires, while also exceeding requirements of J_e and I_c at 20 T. Thinner cores may result in higher bending flexibility and J_e but will reduce I_c at 20 T and will likely reduce their resilience against transverse compressive stress [24].

5. Conclusions

This paper introduces the next generation of CORC® wires wound from production REBCO tapes. The CORC® wires were developed for high-field magnet applications and were produced using optimized lubricants and manufacturing procedures to minimize friction between tapes. The bending performance of CORC® wires wound from 30 REBCO production tapes of 2 mm width that contain 30 μm thick substrates was improved by a factor of more than 2 compared to the previous generation CORC® wires. CORC® wires wound from SP HM production tapes maintained 92.4% of their critical current at 31.5 mm bending radius, while CORC® wires containing 30 tapes from SST maintained 97.5% of their I_c at a 20 mm bending radius and 83.5% of I_c at a 15 mm bending radius. The lower mechanical resilience of tapes from SO to axial compressive winding strain required the use of 3.2 mm thick cores in the CORC® wire, instead of the standard 2.5 mm thick cores. CORC® wires wound from SO tapes maintained 86.5% of their I_c at a bending radius of 25 mm.

The performance of CORC® wires was measured in a background magnetic field up to 12 T in liquid helium. The CORC® wire performance was compared to that of single tape I_c at 4.2 K up to 15 T from tapes of the same batches form which the CORC® wires were wound. A new record J_e, extrapolated to 20 T, of 530 A mm^{-2} at a current of 5.8 kA was achieved in a CORC® wire wound from SP HM tapes, which are optimized for high field operation. The CORC® wire performance was within 90% of the total tape I_c, while bent into a 31.5 mm radius hairpin. A CORC® wire wound from SST tape, which are not yet optimized for high field operation, achieved a J_e, extrapolated to 20 T of 465 A mm^{-2} while bent to 20 mm radius. It also performed well within 90% of the expected I_c. The in-field performance of a CORC® wire wound from 30 SO tapes, in which a 3.2 mm core was used instead of the standard 2.5 mm core, was lower due to the higher conductor thickness. A J_e, extrapolated to 20 T of 388 A mm^{-2} was measured. The CORC® wire J_e extrapolated to 20 T thus increased by a factor of 1.5–1.8 compared to previous generation CORC® wires wound from production REBCO tapes.

Next generation CORC® wires wound from production REBCO tapes now represent the first REBCO-based cable that exceeds all the main requirements for low-inductance, high-field accelerator magnets. They allow bending in all directions to radii below 20 mm while maintaining more than 90% of their performance, demonstrated an engineering current density exceeding 500 A mm^{-2}, and I_c exceeding 5 kA, extrapolated to 20 T. Next generation CORC® wires now enable a more expediated development of low-inductance particle accelerator magnets that generate a dipole field exceeding 20 T

and low-inductance, high-field solenoid magnets generating an axial field as high as 40 T.

Data availability statement

All data that support the findings of this study are included within the article (and any supplementary files).

Acknowledgments

This work is supported by the U.S. Department of Energy, Office of Science, under Award Numbers DE-SC0014009, DE-SC0018127 and DE-SC0024159.

ORCID iDs

Danko van der Laan https://orcid.org/0000-0001-5889-3751
Jeremy Weiss https://orcid.org/0000-0003-0026-3049
Kyle Radcliff https://orcid.org/0009-0002-6389-2176
Dmytro Abraimov https://orcid.org/0000-0002-0587-4917

References

[1] Wang X, Caspi S, Dietderich D R, Ghiorso W B, Gourlay S A, Higley H C, Lin A, Prestemon S O, van der Laan D and Weiss J D 2018 A viable dipole magnet concept with REBCO CORC® wires and further development needs for high-field magnet applications *Supercond. Sci. Technol.* **31** 045007
[2] McIntyre P and Sattarov A 2005 On the feasibility of a tripler upgrade for the LHC *Proc. Particle Accelerator Conf.* pp 634–6
[3] Rossi L and Todesco E 2005 Conceptual design of 20 T dipoles for high-energy LHC (arXiv:1108.1619)
[4] Todesco E, Bottura L, De Rijk G and Rossi L 2014 Dipoles for high-energy LHC *IEEE Trans. Appl. Supercond.* **24** 4004306
[5] Gupta R *et al* 2015 Hybrid high-field cosine-theta accelerator magnet R&D with second-generation HTS *IEEE Trans. Appl. Supercond.* **25** 4003704
[6] Ferracin P *et al* 2023 Conceptual design of 20 T hybrid accelerator dipole magnets *IEEE Trans. Appl. Supercond.* **33** 4002007
[7] Shen T *et al* 2022 Design, fabrication, and characterization of a high-field high-temperature superconducting Bi-2212 accelerator dipole magnet *Phys. Rev. Accel. Beams* **25** 122401
[8] Shen T *et al* 2019 Stable, predictable and training-free operation of superconducting Bi-2212 rutherford cable racetrack coils at the wire current density of 1000 A/mm^2 *Sci. Rep.* **9** 10170
[9] Jiang J, Starch W L, Hannion M, Kametani F, Trociewitz U P, Hellstrom E E and Larbalestier D C 2011 Doubled critical current density in Bi-2212 round wires by reduction of the residual bubble density *Supercond. Sci. Technol.* **24** 082001
[10] Goldacker W, Nast R, Kotzyba G, Schlachter S I, Frank A, Ringsdorf B, Schmidt C and Komarek P 2006 High current DyBCO-ROEBEL assembled coated conductor (RACC) *J. Phys.: Conf. Ser.* **43** 901
[11] Goldacker W, Grilli F, Pardo E, Kario A, Schlachter S I and Vojenčiak M 2014 Roebel cables from REBCO coated conductors: a one-century-old concept for the superconductivity of the future *Supercond. Sci. Technol.* **27** 093001
[12] Takayasu M, Chiesa L, Bromberg L and Minervini J V 2011 Cabling method for high current conductors made of HTS tapes *IEEE Trans. Appl. Supercond.* **21** 2340–4
[13] Takayasu M, Chiesa L, Bromberg L and Minervini J V 2012 HTS twisted stacked-tape cable conductor *Supercond. Sci. Technol.* **25** 014011–21
[14] Otten S, Dhallé M, Gao P, Wessel W, Kario A, Kling A and Goldacker W 2015 Enhancement of the transverse stress tolerance of REBCO roebel cables by epoxy impregnation *Supercond. Sci. Technol.* **28** 065014
[15] Kirby G A *et al* 2017 First cold powering test of REBCO roebel wound coil for the EuCARD2 future magnet development project *IEEE Trans. Appl. Supercond.* **27** 1–7
[16] Rossi L *et al* 2018 The EuCARD2 future magnets program for particle accelerator high-field dipoles: Review of results and next steps *IEEE Trans. Appl. Supercond.* **28** 4001810
[17] van Nugteren J *et al* 2018 Powering of an HTS dipole insert-magnet operated standalone in helium gas between 5 and 85 K *Supercond. Sci. Technol.* **31** 065002
[18] van der Laan D C 2009 $YBa_2Cu_3O_{7-\delta}$ coated conductor cabling for low ac-loss and high field magnet applications *Supercond. Sci. Technol.* **22** 065013
[19] van der Laan D C, Weiss J D and McRae D M 2019 Status of CORC® cables and wires for use in high-field magnets and power systems a decade after their introduction *Supercond. Sci. Techno.l* **32** 033001
[20] Weiss J D, Mulder T, ten Kate H J J and van der Laan D C 2017 Introduction of CORC® wires: highly flexible, round high-temperature superconducting wires for magnet and power transmission applications *Supercond. Sci. Technol.* **30** 014002
[21] Weiss J D, van der Laan D C, Hazelton D, Knoll A, Carota G, Abraimov D, Francis A, Small M A, Bradford G and Jaroszynski J 2020 Introduction of the next generation of CORC® wires with engineering current density exceeding 650 Amm^{-2} at 12 T based on superpower's ReBCO tapes containing substrates of 25 μm thickness *Supercond. Sci. Technol.* **33** 044001
[22] Wang X *et al* 2021 Development and performance of a 2.9 Tesla dipole magnet using high-temperature superconducting CORC® wires *Supercond. Sci. Technol.* **34** 015012
[23] Kar S, Sai Sandra J, Luo W, Kochat M, Jaroszynski J, Abraimov D, Majkic G and Selvamanickam V 2019 Next-generation highly flexible round REBCO STAR wires with over 580 A mm−2 at 4.2 K, 20 T for future compact magnets *Supercond. Sci. Technol.* **32** 10LT01
[24] van der Laan D C, McRae D M and Weiss J D 2019 Effect of transverse compressive monotonic and cyclic loading on the performance of superconducting CORC® cables and wires *Supercond. Sci. Technol.* **32** 015002
[25] Galstyan E *et al* 2023 High critical current STAR® wires with REBCO tapes by advanced MOCVD *Supercond. Sci. Technol.* **36** 055007
[26] Wang X *et al* 2022 An initial magnet experiment using high-temperature superconducting STAR® wires *Supercond. Sci. Technol.* **35** 125011
[27] Castaneda N *et al* 2024 A 6-around-1 cable using high-temperature superconducting STAR® wires for magnet applications *Supercond. Sci. Technol.* **37** 035009
[28] van der Laan D C *et al* 2020 A CORC® cable insert solenoid: the first high-temperature superconducting insert magnet tested at currents exceeding 4 kA in 14 T background magnetic field *Supercond. Sci. Technol.* **33** 05LT03

[29] Wang X, Dietderich D R, DiMarco J, Ghiorso W B, Gourlay S S A, Higley H C, Lin A, Prestemon S O, van der Laan D C and Weiss J D 2019 A 1.2-T canted cos θ dipole magnet using high-temperature superconducting CORC® wires *Supercond. Sci. Technol.* **32** 075002

[30] Anvar V A *et al* 2018 Bending of CORC® cables and wires: finite element parametric study and experimental validation *Supercond. Sci. Technol.* **31** 115006

[31] Anvar V A, Wang K, Weiss J D, Radcliff K, van der Laan D C, Hossain M S A and Nijhuis A 2022 Enhanced critical axial tensile strain limit of CORC® wires: FEM and analytical modeling *Supercond. Sci. Technol.* **35** 055002

[32] van der Laan D C, McRae D M and Weiss J D 2019 Effect of monotonic and cyclic axial tensile stress on the performance of superconducting CORC® wires *Supercond. Sci. Technol.* **32** 054004